Zeitschrift: Schweizerische mineralogische und petrographische Mitteilungen = Bulletin suisse de minéralogie et pétrographie

Band: 81 (2001)

Heft: 3: Monte Rosa nappe

Artikel: Geochemistry of a talc-kyanite-chloritoid shear zone within the Monte Rosa granite, Val d'Ayas, Italy

Autor: Pawlig, Sabine / Baumgartner, Lukas P.

DOI: https://doi.org/10.5169/seals-61696

SCHWEIZ. MINERAL. PETROGR. MITT. 81, 329–346, 2001

Dedicated to the memory of Prof. Martin Frey

Geochemistry of a talc-kyanite-chloritoid shear zone within the Monte Rosa granite, Val d'Ayas, Italy

by *Sabine Pawlig*[1*] and *Lukas P. Baumgartner*[1#]

Abstract

Kyanite-talc-chloritoid-bearing rocks are exposed in a shear zone and other places within the Monte Rosa granite in the upper Val d'Ayas (Italy). Weakly deformed granite grades into progressively more deformed gneiss and whiteschist. A garnet-talc-chloritoid-calcite-pyrite-quartz boudin marks the center of this shear zone. The occurrence of weakly deformed whiteschists and discordant whiteschist-granite contacts indicates a pre-deformation origin of the whiteschist chemistry. Mass balance calculations were done in order to assess the nature and amount of mass transfer necessary to produce the whiteschist from a granitic protolith. The results indicate enrichment of Mg and H_2O, with minor Si, Fe and K. Na, Ca, Sr, Ba, Pb and locally U are depleted. Stable isotope investigations on calcite from the carbonate zone in the center of the shear zone were performed to constrain the fluid source. $\delta^{13}C$ values of calcite range from –9.60 to –9.81‰ (PDB), while their $\delta^{18}O$ values range from +9.61 to +10.14‰ (VSMOW). These light isotopic values point towards a magmatic fluid source. We suggest that a pre-Alpine argillitic alteration leads to a chlorite-rich metasomatic alteration of the granite around gangue mineralization. Strain was localized during high-pressure metamorphism and subsequent exhumation into these rocks. This formed a deformational weak zone in the otherwise dry Monte Rosa granite. The presence of hydrous phases prior to metamorphism led to abundant recrystallization during high-pressure metamorphism.

Keywords: Monte Rosa nappe, whiteschist, metasomatism, ISOCON, stable isotope geochemistry.

Introduction

Talc-chloritoid-kyanite-bearing rocks are found in discrete shear zones within the Late Permian Monte Rosa granite, Western Alps (Fig. 1a). Occurrences of these rocks in the Monte Rosa nappe were already described by BEARTH (1952) and DAL PIAZ (1971). Petrological investigations on those phengite-talc-chloritoid-chlorite-kyanite-quartz assemblages from the Monte Rosa nappe in the Val d'Ayas (Italy) were carried out by CHOPIN and MONIÉ (1984), and DAL PIAZ and LOMBARDO (1986), who reported a pressure of ca. 16 kbar at a temperature of 500 °C for their formation at a water activity of approximately 0.6 during the Alpine eclogitic overprint. Recently, LE BAYON et al. (2000) suggested a considerably higher pressure of 25 kbar and a temperature of 580 °C for the stability of the assemblage talc-chloritoid within rocks from the Monte Rosa nappe based on an assumed water activity of 0.6 during the Alpine high-pressure metamorphism. A sedimentary origin for those special rocks was suggested by CHOPIN and MONIÉ (1984) for a piece of the float, whereas several authors proposed that these peculiar rocks resulted from pre- to early Alpine metasomatic transformations of the granitic protolith along high-pressure shear zones in the Monte Rosa granite (BEARTH, 1952; DAL PIAZ, 1971; DAL PIAZ and LOMBARDO, 1986). Occurrences of similar rock types in the Alps have been reported from the Tauern Window of Austria, the Austroalpine nappes of the Eastern Alps (Hungary), and from the coesite-bearing rocks of the Dora Maira massif in the Western Alps (ABRAHAM et al.,

[1] Institut für Geowissenschaften, Mineralogie, Johannes Gutenberg-Universität, Saarstr. 21, D-55099 Mainz.
* Present address: GZG – Göttinger Zentrum Geowissenschaften, Abt. Isotopengeologie, Georg-August-Universität, Goldschmidtstr. 3, D-37077 Göttingen. <spawlig@gwdg.de>
# Present address: Institut de Minéralogie et Pétrographie, Université de Lausanne, BFSH 2, CH-1015 Lausanne.

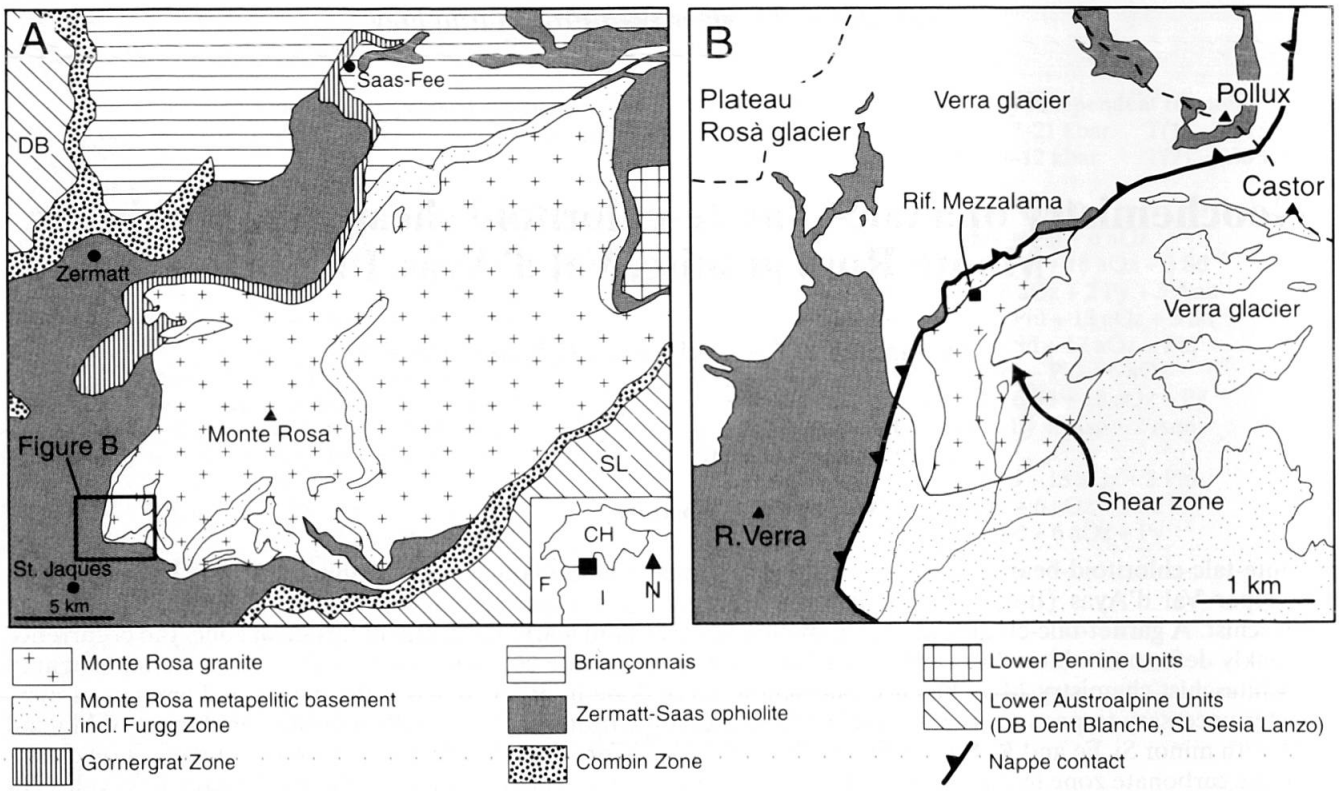

Fig. 1 (A) Generalized map of study area showing the Monte Rosa nappe and surrounding tectonic units (modified after BEARTH, 1952). (B) Map of the upper Val d'Ayas indicates location of the shear zone (arrow). Modified after DAL PIAZ (1971).

1974; CHOPIN et al., 1991; SHARP et al., 1993; DEMÈNY et al., 1997). Two different mechanisms have been proposed for the formation of Alpine whiteschists: high-pressure metamorphic overprint of Mg-rich evaporitic sedimentary protoliths (CHOPIN and MONIÉ, 1984), and Mg-metasomatism of gneisses and mica schists along shear zones by metamorphic fluids (SHARP et al., 1993). A stable isotope study was presented by SHARP et al. (1993), in which they proposed that the metasomatic alteration was caused by ascending metamorphic fluids released from the subducted mafic to ultramafic material of the Tethyan oceanic crust of the downgoing slab.

This study focuses on the geochemical evolution of a shear zone containing whiteschists located in an otherwise weakly deformed part of the Monte Rosa granite in the upper Val d'Ayas (Italy). Field and petrographic observations described below provide clear evidence that the whiteschists are the result of a high-pressure metamorphic overprint of a hydrothermally altered granitic protolith and related microgranitic dykes. To constrain the nature and amount of the mass transport necessary to produce these special rocks from a granitic protolith, the approach of BAUMGARTNER and OLSEN (1995) based on the ISOCON method after GRANT (1986) and GRESENS (1967) was applied. Using carbon and oxygen stable isotope geochemistry of calcite from a garnet-talc-chloritoid-calcite-pyrite-quartz zone located in the center of this shear zone, we address the potential fluid source and the evolution of these magnesian rocks within the shear zone.

Geology and petrography of the talc-kyanite-chloritoid shear zone in the upper Val d'Ayas

The shear zone investigated in this study is located in a weakly deformed part of the Monte Rosa granite in the upper part of the Val d'Ayas (Italy). It is located southeast of the Mezzalama refuge, at the southern end of the Verra glacier (Fig. 1b; 2796 m a.s.l.; coordinates 625.05/084.143, Swiss kilometric grid). The shear zone is up to 40 m wide, trends NW–SE and dips towards WSW (250/40). The weakly deformed granite grades into more deformed granitic gneiss and finally into a chloritoid-kyanite-talc-bearing whiteschist (Figs 2, 3). Microgranitic dykes were rotated into the shear zone (Fig. 4a), indicating a downward movement of the hangingwall (top towards the SW). A small boudin (2.5 m × 1 m) containing

garnet-talc-chloritoid-phengite-calcite-pyrite-quartz forms the center of the shear zone (Fig. 2). The orientation of both, the whiteschist and the carbonate boudin in the center, is slightly oblique to the generally NW–SE trending southwestern rim of the shear zone. Additionally, a discordant contact of the whiteschist with the Monte Rosa granite can be observed at the eastern rim of the shear zone, whereby the main foliation of the rocks clearly cuts the contact between the two different lithologies (Fig. 2). Two detailed profiles document sample location, lithological units and structural data (Fig. 3).

Weakly deformed, nearly massif lenses and boudins of chloritoid-talc felses occur just below the carbonate boudin, indicating an initial near-static crystallization during high-pressure metamorphism. Shearing continued into the greenschist-facies, which is documented by some C-type shear bands containing chlorite, muscovite, and locally biotite in the whiteschist (Fig. 4d). The last structural elements within the shear zone are extensional quartz veins, along which intensive alteration of gneisses and whiteschists by chlorite, muscovite and some biotite is observed (Fig. 3, section C–D). These late quartz veins are at high angle to the shear zone. A similar succession of deformation fabrics and metamorphic assemblages is observed for the granitic gneiss. Sigma clasts of feldspar in the granitic gneiss (Fig. 4c) define a downward movement of the hangingwall (top towards the SW), as do the C-type shear bands within the whiteschists (Fig. 4d). Elongate feldspar and white mica aggregates, as well as prismatic, broken tourmaline crystals define a SW-trending (220/40) stretching lineation in the gneiss (Fig. 3). The tourmaline lineation occurs within whiteschists and microgranitic dykes as well. Chlorite, low-celadonitic white mica and minor biotite replace phengite, which defines the

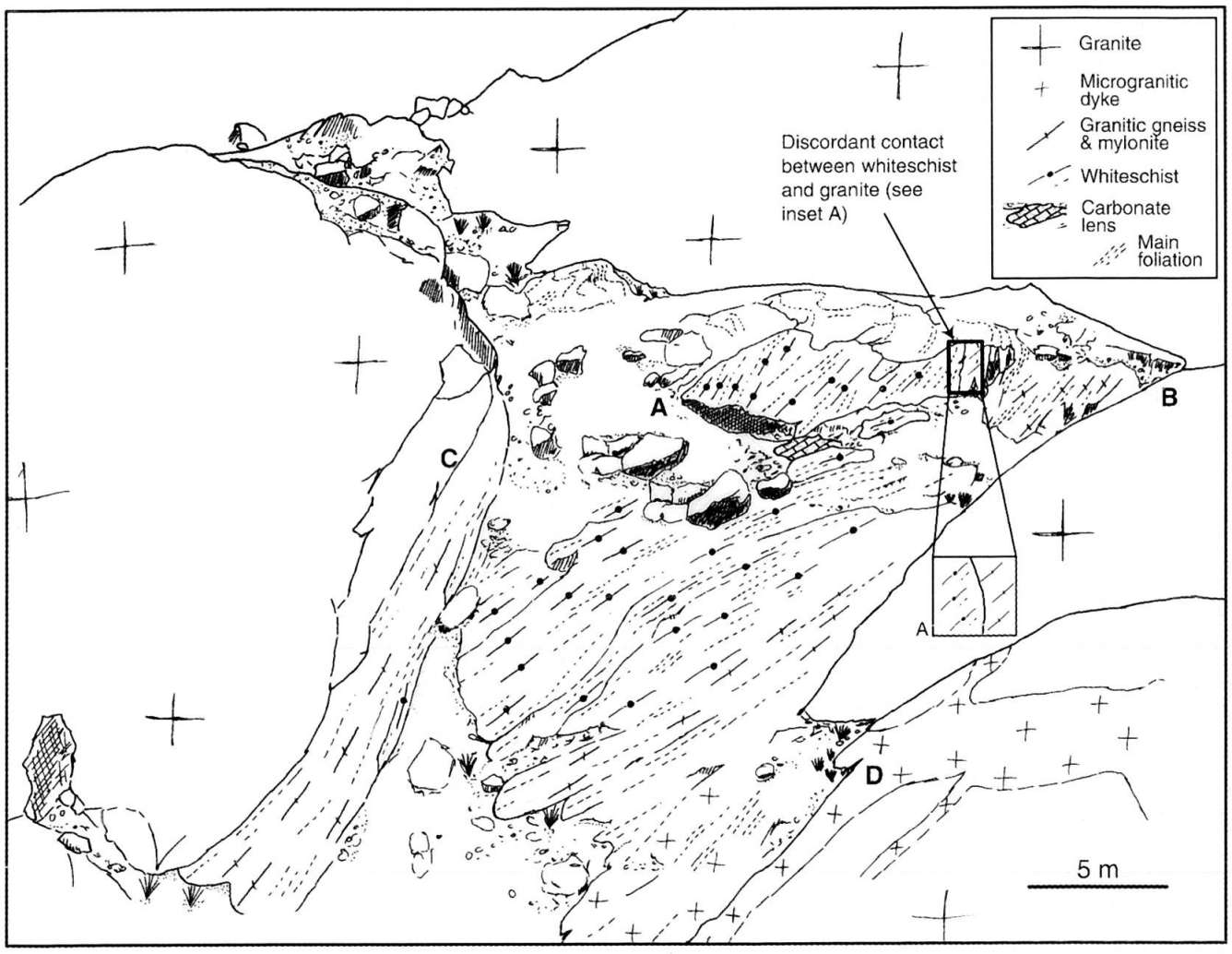

Fig. 2 Sketch of the shear zone located at 625.05/084.143 (Swiss kilometric grid). The view is towards NW. The locations of the sections A–B and C–D in figure 3 are indicated. Note the carbonate boudin located just east of the center and the discordant contact between the whiteschist and the granite as indicated by the arrow. Detail of contact given in inset A.

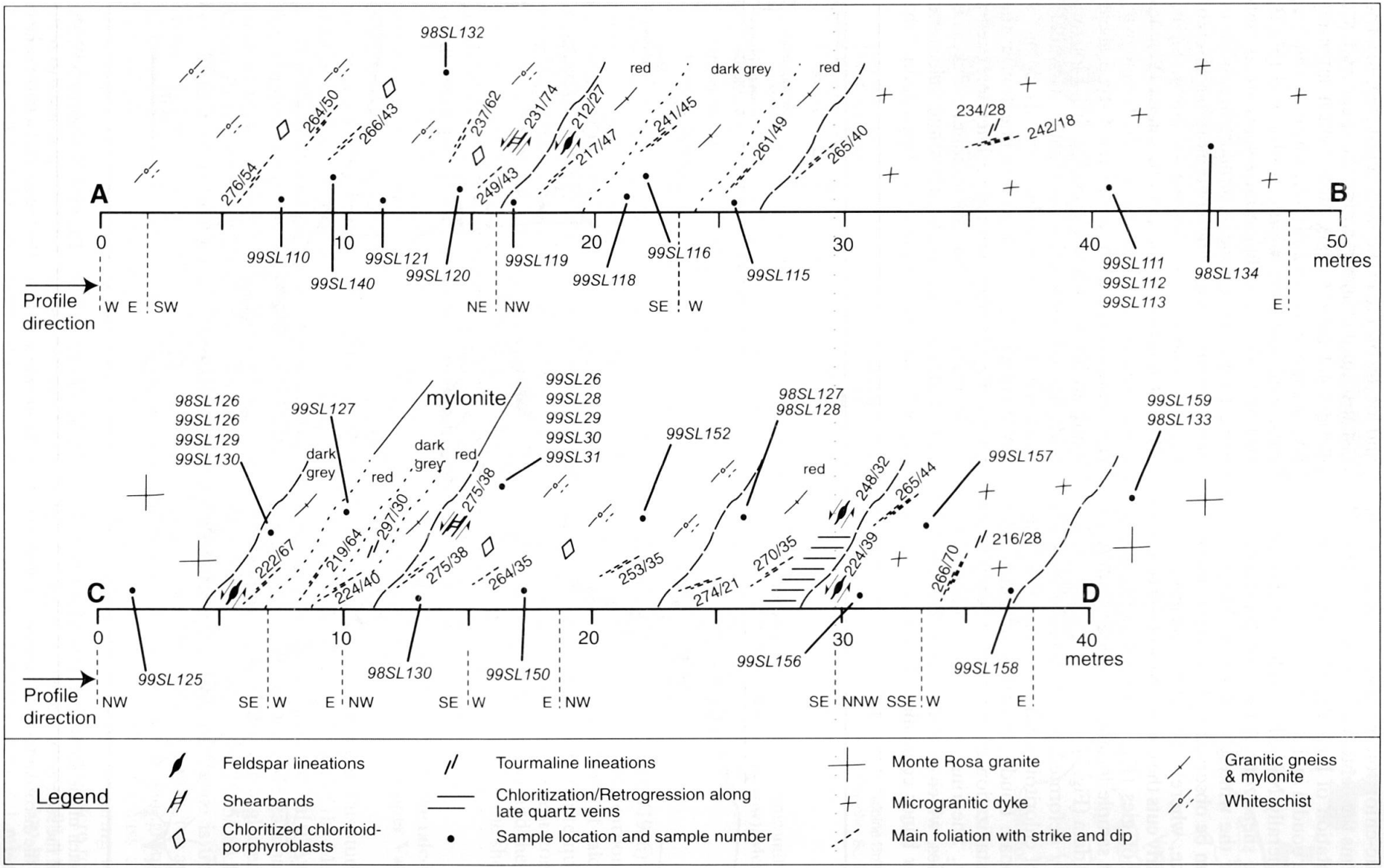

Fig. 3 SW–NE cross sections (locations indicated in figure 2) across the shear zone drawn with structural informations and sample locations. Section C–D in south-eastern part of the shear zone covers the whole sequence of rocks occurring within the shear zone, with the exception of the carbonate boudin.

earliest foliation together with talc in the whiteschist. All structural elements, except the late quartz veins, document a top-to-SW sense of shear with downward movement of the hangingwall. The characteristics of the deformation fabrics within the different lithologies, i.e within the granitic gneiss and the whiteschist, demonstrate that deformation in the shear zone prevailed continuously from at least the last stages of high-pressure metamorphism to the greenschist-facies overprint.

The weakly deformed, slightly foliated Monte Rosa granite shows a well preserved igneous texture which is dominated by large K-feldspar blasts, large biotite and muscovite flakes, and quartz. Igneous plagioclase is replaced pseudomorphically by aggregates of fine-grained phengite, garnet, clinozoisite, and fine-grained albite. Relict magmatic biotite locally contains sagenite inclusions. Biotite is either overgrown by fine-grained phengite at its rims or, locally replaced by chlorite. Accessory apatite, ilmenite (partially rimmed by titanite), zircon, monazite, xenotime and tourmaline are common. Weakly deformed dykes occur, characterized by a granoblastic texture, consisting of quartz, plagioclase, muscovite, phengite, clinozoisite, small garnet, as well as minor tourmaline and zircon. Relictic, magmatic muscovite flakes are replaced by fine-grained phengite at the rim, whereas the plagioclase shows replacement by an assemblage of phengite-clinozoisite-garnet-albite, similar to that reported for the metagranite.

Metagranite grades within a few centimeters into the shear zone, which starts with two slightly different varieties of granitic gneiss: a dark gray and a red one. The main constituents of both varieties of granitic gneiss are large augen-like feldspar clasts, quartz, phengite, chlorite, and epidote. Small garnet displays atoll structures. Biotite can form thin rims on chlorite and phengite. Minor constituents and accessory phases include zircon, apatite, rutile and titanite. Small amounts of tourmaline occur locally within the red gneiss. Phengite, biotite and epidote are concentrated in layers, defining the main foliation of this rock type, or they wrap around feldspar clasts and oblate quartz aggregates. The two granitic gneisses form alternating layers in the cross section A–B. The red variety is largely of mylonitic character and mainly observed towards the center of the shear zone and in direct contact with the whiteschist in section C–D (Fig. 3).

Whiteschists contain the assemblage kyanite-talc-chloritoid-phengite-quartz, with minor amounts of rutile, tourmaline, pyrite, monazite, and zircon. Phengite and talc define the first foliation. The chloritoid-porphyroblasts are up to one cm in size and chloritoid is sometimes intergrown with kyanite to form large aggregates that are also up to one cm in size. This assemblage is partially replaced by the assemblage of chlorite-muscovite and sometimes biotite. Tourmaline occurs either as small grains, or as prisms defining the lineation. Two different protoliths for the whiteschist can be distinguished in the field. One clearly has a granitic protolith and is characterized by large chloritoid, whereas the other, very light variety, with only minor chloritoid, originates from microgranitic dykes. They are separated by sharp contacts parallel to the direction of the shear zone.

In the center of the shear zone, a sulfide-bearing carbonate boudin has been found (Figs 2, 4b). It is only slightly foliated, found in sharp contact to whiteschists and oriented parallel to the foliation of the whiteschists, which is slightly oblique to the shear zone. The sharp contact to the whiteschists suggests that the carbonate boudin represents a vein mineralization. It contains the assemblage chloritoid-talc-garnet-phengite-quartz-calcite-pyrite±chalcopyrite. Pyrite and chalcopyrite occur as stringes within the carbonate boudin. Accessory phases are monazite, allanite (from 100 μm to several cm in size), zircon and rutile. Massive, nearly pure carbonate layers with minor quartz and phengite show a sharp contact to layers rich in quartz, chloritoid, garnet, phengite, talc and pyrite with minor carbonate. Talc and phengite define the slight foliation of the samples. They are bend around large chloritoid and garnet crystals. Signs of greenschist-facies retrogression within the carbonate boudin are given by the presence of chlorite, muscovite, and incipient biotite, which occurs as narrow rims around the phengites. Textural relationships of monazites imply that they formed or recrystallized during Alpine metamorphism. They are mainly found within the foliation and occur either as large, single grains or as a number of small grains pseudomorphically replacing larger ones. Several large, unzoned monazite grains from a sample of the carbonate zone yielded $^{208}Pb/^{232}Th$ ages between 39 ± 0.9 and 31.6 ± 0.7 Ma (SCHERRER, 2001), and thus provide clear evidence for monazite recrystallization within the shear zone during Alpine metamorphism and deformation.

Combining the textural and geochronological observations of monazites from the carbonate zone with field and petrographic observations from the whiteschist and granitic gneiss it is therefore clear that the shear zone is of Alpine age and provides essential evidence of a high-pressure metamorphic overprint within the Monte Rosa nappe.

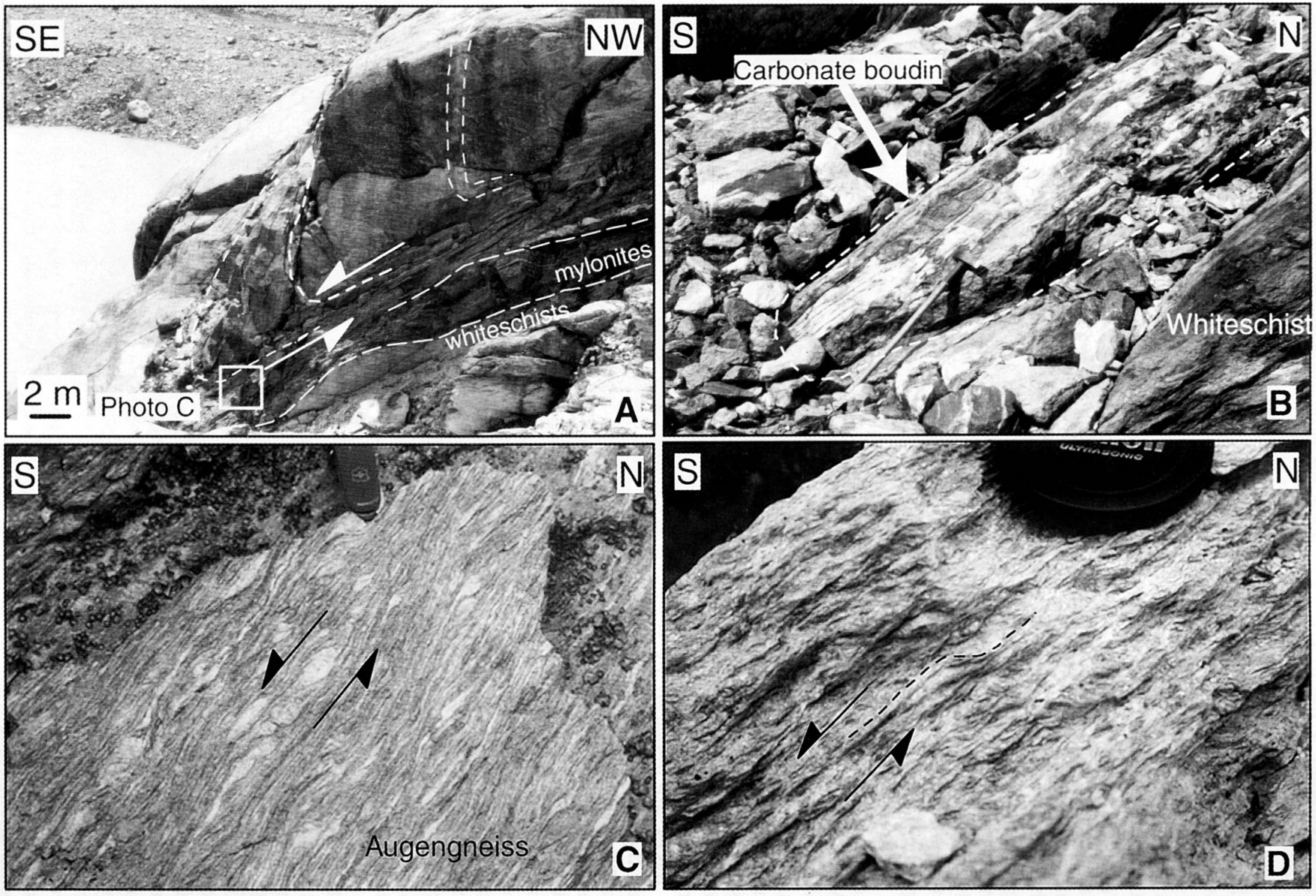

Fig. 4 Detailed photographs of the shear zone. (A) The bottom of this wall shows strongly foliated whiteschists, followed upwards by a layer of mylonite. The microgranitic dykes are sheared into the augengneiss zone of the "grey" granitic gneisses (the locality of photo C is indicated). (B) The central carbonate boudin (note hammer of 60 cm length for scale). (C) Sigmoidal feldspar porphyroclasts in granitic gneiss in section C–D from the western edge of the shear zone. (D) Shear bands within the whiteschist in section C–D.

Analytical methods

Whole rock chemical compositions were determined by XRF measurements. Samples were crushed and powdered in a tungsten carbide mill. Major element concentrations were measured on glass pellets, while trace elements were determined on powder pellets, using a Philips PW 1400 spectrometer with a rhodium X-ray tube. LOI (loss on ignition) was calculated from weight loss by heating whole rock powders to 1000 °C for at least two hours. LOI is assumed to be H_2O, since the shear zone rocks, with the exception of the carbonate zone within the center of the shear zone, do not contain any CO_2-bearing minerals. The mean for each sample population is given in table 1 with the 1σ standard deviation, calculated from multiple samples of each rock population. The numbers of samples varies between 3 to 8 for the different lithologies occurring within the shear zone (see Tab. 1).

$^{18}O/^{16}O$ and $^{13}C/^{12}C$ ratios were determined from CO_2-gas, liberated from calcite by reaction with 100% phosphoric acid at 25 °C. Isotopic ratios were analyzed with a VG ISOTECH-PRISM SERIES II mass spectrometer. All values are given relative to PDB standard for $\delta^{13}C$ and VSMOW standard for $\delta^{18}O$, respectively. Uncertainties of the isotopic ratios for carbon and oxygen are 0.05‰ and 0.1‰ (1σ), respectively. Stable isotope compositions of the analyzed samples are given in table 3.

Mass balance calculations

Quantitative mass balance calculations based on chemical data requires an assumption with respect to volume or mass change during the alteration process (GRESENS, 1967; GRANT, 1986; BAUMGARTNER and OLSEN, 1995). Typically it is not possible to obtain this information unequivocally from field observations, hence alternative routes are used. In the literature, the assumptions of constant volume or immobile elements are commonly used (e.g. AGUE, 1994, 1997; BAUMGARTNER and OLSEN, 1995; GRANT 1986; OLSEN and GRANT, 1991). Once a choice has been made, evaluation of mass transport is calculated with the approach of GRESENS (1967), or its graphical simplification of GRANT (1986). The graphical approach pioneered by GRANT (1986) is referred to as the ISOCON method: The concentrations of the elements in the metasomatized rock are plotted versus the concentrations of the least-altered equivalent. The concentrations of all immobile species must lie on a straight line (GRESENS, 1967; GRANT, 1986):

$$c_i^A = \frac{M^O}{M^A}\left[c_i^O + \Delta c_i\right] \quad (1)$$

where M^O and M^A are the masses of the original and the altered rock in an equal-sized volume of rock, respectively; c_i^O and c_i^A are the concentrations of element i in the original and in the altered rock, respectively; and Δc_i is the mass change of element i during the alteration process. The line connecting all elements with no mass change ($\Delta c_i = 0$) is called an ISOCON. Its slope, $b = M^O/M^A$, corresponds to the overall mass ratio, which resulted from the alteration process. A significant deviation of data points from the ISOCON is due to the mass change of the corresponding element during alteration. A mass ratio of one ($b = 1$) demonstrates that no overall mass change has taken place during the alteration process, whereas $b < 1$ indicates mass gain, and $b > 1$ indicates mass loss. BAUMGARTNER and OLSEN (1995) presented a least-squares approach to the ISOCON method of GRANT (1986) which takes into account the heterogeneity of the original (parent) and metasomatized (altered) rock population. The method is statistically rigorous, if the heterogeneities of the altered and the parent rock population are described either by a normal or a log-normal distribution. Also, its current implementation assumes that no correlation between the two populations is observed. In practice, inhomogeneities and analytical errors are evaluated through multiple analyses of different samples from one rock population. It is thus possible to obtain the associated uncertainties of the original and the altered rock population for each element. Since sample populations are typically too small to test for the type of distribution, a normal or log-normal distribution is assumed. Here, the results are presented in log-log diagrams, where the concentration of an element i in the altered rock c_i^A is related to the concentration in the original rock c_i^O by rearranging equation (1) to:

$$\log c_i^A = \log \frac{M^O}{M^A} + \log(c_i^O + \Delta c_i) \quad (2)$$

and hence for the ISOCON defining the immobile elements

$$y = \log \frac{M^O}{M^A} + \log c_i \quad (3)$$

The slope of the ISOCON in a log-log diagram is always one. The amount of overall mass change is given by the deviation of the intercept value of the ISOCON from the origin.

Tab. 1 Chemical composition of the shear zone samples used for the mass balance calculations. Average compositions and their 1σ variability is shown for multiple samples of different shear zone lithologies.

Rock type	**Monte Rosa Granite**					**Dark grey variety of the granitic gneiss**						
Sample	98SL133	99SL125	99SL159	Mean	1 σ	98SL126	99SL118	99SL126	99SL129	99SL130	Mean	1 σ
SiO_2 **wt%**	69.77	70.46	70.5	70.24	0.41	70.37	69.83	70.42	69.8	70.76	70.20	0.47
Al_2O_3	15.3	14.93	14.73	14.99	0.29	14.72	14.89	14.64	14.61	14.55	14.67	0.15
Fe_2O_3*	2.66	2.88	3.03	2.86	0.19	3.18	3.07	3.06	3.14	3.12	3.10	0.04
MnO	0.05	0.05	0.05	0.05	0.00	0.05	0.05	0.06	0.05	0.05	0.05	0.00
MgO	0.74	0.78	0.82	0.78	0.04	0.86	0.85	0.85	0.87	0.83	0.85	0.02
CaO	1.57	1.79	1.68	1.68	0.11	1.76	1.65	1.79	1.71	1.73	1.72	0.06
Na_2O	3.11	3.21	3.1	3.14	0.06	2.96	3.11	3.71	2.92	2.93	3.17	0.37
K_2O	5.25	4.3	4.56	4.70	0.49	4.61	3.99	2.84	4.93	4.77	4.13	0.95
TiO_2	0.41	0.44	0.47	0.44	0.03	0.5	0.51	0.48	0.49	0.48	0.49	0.01
P_2O_5	0.21	0.2	0.19	0.20	0.01	0.18	0.2	0.18	0.18	0.18	0.19	0.01
LOI	1.01	1.18	0.99	1.06	0.10	1.41	1.62	1.63	1.19	1.22	1.42	0.24
Total	100.06	100.23	100.12	100.14	0.09	100.6	99.77	99.66	99.89	100.62	99.99	0.43
Sc **ppm**	5	5	6	5.3	0.6	4	6	5	5	4	5	0.8
V	24	25	30	26.3	3.2	31	34	31	30	30	31.3	1.9
Cr	18	9	12	13.0	4.6	13	8	10	9	10	9.3	1.0
Co	51	41	42	44.7	5.5	26	27	26	38	40	32.8	7.3
Ni	7	5	4	5.3	1.5	9	7	7	7	6	6.8	0.5
Cu	8	10	7	8.3	1.5	6	8	5	11	7	7.8	2.5
Zn	54	48	53	51.7	3.2	59	58	46	59	59	55.5	6.4
Ga	19.3	17.6	19	18.6	0.9	18	19.2	18	18	19	18.6	0.6
Rb	248	183	225	218.7	33.0	209	200	151	214	224	197.3	32.4
Sr	124	116	110	116.7	7.0	103	84	108	109	105	101.5	11.8
Y	20	22	24	22.0	2.0	24	24	25	25	22	24.0	1.4
Zr	153	162	174	163.0	10.5	173	175	166	166	169	169.0	4.2
Nb	16	15	16	15.7	0.6	16	17	15	15	17	16.0	1.2
Ba	594	429	433	485.3	94.1	481	382	407	498	416	425.8	50.3
Pb	34.3	33.6	30.7	32.9	1.9	28.1	32.9	16.2	26.8	37.8	28.4	9.3
Th	14.3	15.9	14.3	14.8	0.9	17.4	16.6	15.3	16.5	16.4	16.2	0.6
U	4.3	4.7	4.7	4.6	0.2	4.2	3.1	4	3.8	4.5	3.9	0.6
La	25	27	32	28.0	3.61	28	31	27	31	28	29.0	1.9
Ce	43	49	59	50.3	8.08	59	61	56	63	60	59.8	2.6
Pr	7	10	8	8.3	1.53	6	9	5	8	9	7.4	1.8
Nd	24	27	27	26.0	1.73	28	32	27	30	28	29.0	2.0
Sm	4	8	5	5.7	2.08	5	6	7	5	5	5.6	0.9

* Total Fe shown as Fe_2O_3; Fe^{2+}/Fe^{3+} not determined.

Mass balance calculations were performed for the alteration, using the Monte Rosa granite as the original rock type of the shear zone for calculations concerning the alteration towards the granitic gneiss and the whiteschist with granitic origin. The microgranitic dyke is the original rock type for the calculations of the alteration towards the whiteschist with microgranitic origin. The ISOCON was chosen, so as to have a maximum number of elements assumed to have low-solubility, and hence are most likely relatively immobile (Al, Ti, P, Zr, Sc, Y, V). The calculations were performed with the software package „ISOCON" written in FORTRAN 77 (BAUMGARTNER and OLSEN, 1995). Whole rock chemical data as well as their 1σ uncertainty used for the calculations are given in table 1. Note that the data for the REE are especially in the whiteschist and in the microgranitic dykes close to or below the detection limit of the XRF.

An ISOCON plot for the alteration of the Monte Rosa granite to the dark gray variety of the granitic gneiss is shown in figure 5a. For this calculation, the element combination with the maximum number of the previously mentioned generally immobile elements (Al, Ti, P, Sc, Y, Zr, Nb, Th) was chosen to define the ISOCON. Some additional elements are compatible with this ISOCON as well (Tab. 2). The mass balance calculation results in an ISOCON with a mass ratio b = 1.0 ± 0.1, which implies that no overall mass change has taken place during the alteration of the granite to the dark gray granitic gneisses. Most elements scatter around the ISOCON within their uncertainty. Only Mg, H_2O, Fe and Ti plot slightly above the ISOCON, implying enrichment of these elements during the alteration process.

Figure 5b shows an ISOCON plot for the alteration of the granite to the red variety of the granitic gneiss. The red variety of the granitic gneiss is observed towards the center of the shear zone, often in direct contact with the whiteschist (Fig. 3). They are largely mylonites. The alteration to the red variety of the granitic gneiss is character-

Tab. 1 (cont.)

Rock type	**Whiteschists with granitic origin**										**Whiteschists with microgranitic origin**						
Sample	98SL130	98SL132	99SL26	99SL28	99SL29	99SL30	99SL31	99SL140	Mean	1 σ	99SL110	99SL120	99SL121	99SL150	99SL152	Mean	1 σ
SiO_2 **wt%**	71.06	73.62	71.46	69.62	70.4	64.86	70.55	67.48	69.88	2.66	60.9	73.66	71.97	63.68	69.98	68.04	5.50
Al_2O_3	11.25	15.19	14.44	14.81	14.81	15.78	14.99	15.96	14.65	1.47	20.28	14.33	14.94	19.72	15.51	16.96	2.82
Fe_2O_3*	4.22	0.8	1.29	1.47	1.39	3.5	1.62	3.36	2.21	1.28	1.58	1.46	1.77	1.49	1.08	1.48	0.25
MnO	0.04	0.01	0.01	0.01	0.01	0.04	0.01	0.03	0.02	0.01	0.01	0.01	0.02	0.01	0.01	0.01	0.00
MgO	8.21	2.38	4.64	5.3	4.96	7.76	5.11	4.39	5.34	1.87	5.23	2.6	2.74	3.81	4.11	3.70	1.08
CaO	0.09	0.26	0.32	0.28	0.29	0.17	0.22	0.17	0.23	0.08	0.83	0.33	0.38	0.25	0.39	0.44	0.23
Na_2O	0.04	0.31	0.77	0.71	0.81	0.17	0.28	0.15	0.41	0.31	0.34	0.32	0.32	0.41	0.24	0.33	0.06
K_2O	1.31	4.51	3.7	3.75	3.73	3.28	3.62	3.77	3.46	0.93	5.45	3.97	3.84	5.91	4.33	4.70	0.93
TiO_2	0.29	0.06	0.34	0.48	0.42	0.52	0.44	0.43	0.37	0.15	0.05	0.04	0.03	0.52	0.44	0.22	0.24
P_2O_5	0.07	0.19	0.21	0.19	0.2	0.14	0.18	0.13	0.16	0.05	0.62	0.24	0.28	0.19	0.3	0.33	0.17
LOI	4.03	2.87	3.33	3.6	3.42	4.24	3.48	3.56	3.57	0.42	4.3	2.61	2.73	4.03	3.53	3.44	0.76
Total	100.6	100.2	100.51	100.52	100.46	100.47	100.51	99.43	100.34	0.38	99.6	99.58	99.03	100.01	99.92	99.63	0.38
Sc **ppm**	5	3	6	7	4	8	7	8	6.0	1.9	3	2	1	6	4	3.2	1.9
V	21	3	22	30	28	36	28	36	25.5	10.6	3	7	2	20	21	10.6	9.2
Cr	5	0	8	9	7	10	5	16	7.5	4.6	0	0	0	11	11	4.4	6.0
Co	26	23	17	20	23	19	24	16	21.0	3.5	10	28	35	25	23	24.2	9.1
Ni	12	6	6	6	6	9	7	10	7.8	2.3	4	3	3	3	4	3.4	0.5
Cu	4	1005	5	2	4	2	3	7	129.0	354.0	3	4	1	4	4	3.2	1.3
Zn	23	515	16	17	17	20	14	18	80.0	175.8	14	19	32	9	8	16.4	9.8
Ga	12	18	18	19	19	18	19	19.9	17.9	2.5	17.1	18.8	19.3	21	15	18.24	2.3
Rb	63	200	173	168	171	157	160	197	161.1	42.6	235	191	205	270	183	216.8	35.7
Sr	3	11	28	28	29	8	11	8	15.8	10.7	18	19	14	16	12	15.8	2.9
Y	13	6	19	21	19	16	20	25	17.4	5.8	9	5	5	7	9	7	2.0
Zr	109	22	120	171	150	173	148	123	127.0	48.5	26	27	26	195	167	88.2	85.3
Nb	11	8	15	15	15	16	14	15	13.6	2.7	2	12	12	19	12	11.4	6.1
Ba	43	117	90	104	92	87	86	97	89.5	21.4	130	115	100	161	105	122.2	24.5
Pb	3.3	11.4	5.9	5	5.8	3.3	3.8	3.2	5.2	2.7	4.4	4.3	4	4.3	3.6	4.12	0.3
Th	14	1	8.8	13.2	12.3	14.1	12.3	9.4	10.6	4.4	1.8	0.1	0	15.5	13.4	6.16	7.6
U	2.7	0.9	1.7	2.7	2.1	2.8	3.8	2.7	2.4	0.9	0	0.7	3.7	0.8	0.2	1.08	1.5
La	16	0	17	23	25	15	23	4	15.4	9.1	0	0	0	1	2	0.6	0.9
Ce	34	0	28	45	43	30	38	0	27.3	17.8	0	0	0	0	0	0	0.0
Pr	5	0	3	5	4	4	5	1	3.4	1.9	1	2	1	0	0	0.80	0.8
Nd	17	0	15	23	23	14	21	5	14.8	8.4	2	0	0	0	1	0.6	0.9
Sm	2	0	3	5	6	3	5	3	3.4	1.9	3	1	2	3	1	2	1.0

* Total Fe shown as Fe_2O_3; Fe^{2+}/Fe^{3+} not determined.

Tab. 1 (cont.)

Rock type	**Red variety of the granitic gneiss**							**Microgranitic dykes**									
Sample	99SL119	98SL127	98SL128	99SL115	99SL127	Mean	1 σ	98SL134	99SL111	99SL112	99SL113	99SL116	99SL156	99SL157	99SL158	Mean	1 σ
SiO_2 **wt%**	69.71	70.12	69.42	73.08	68.61	70.19	1.71	74.99	74.97	74.97	73.92	75.44	72.64	75.87	74.54	74.67	1.00
Al_2O_3	15.02	15.16	14.85	13.95	15.84	14.96	0.68	14.94	14.48	14.43	14.72	14.71	14.76	14.54	14.49	14.63	0.18
Fe_2O_3*	1.73	1.69	1.91	1.19	1.79	1.66	0.28	0.86	0.67	0.69	0.58	0.86	1.04	0.64	0.89	0.78	0.16
MnO	0.02	0.02	0.03	0.02	0	0.02	0.01	0.03	0.03	0.03	0.02	0.04	0.01	0.03	0.06	0.03	0.01
MgO	5.09	3.72	4.38	3.03	4.02	4.05	0.76	0.23	0.09	0.1	0.09	0.13	2.44	0.11	0.09	0.41	0.82
CaO	0.25	0.33	0.34	0.3	0.33	0.31	0.04	0.86	0.69	0.82	0.62	0.65	0.2	0.68	0.48	0.63	0.21
Na_2O	0.22	0.11	0.11	0.81	0.11	0.27	0.30	4.15	3.97	4.13	3.85	6.21	0.48	4.88	4.14	3.98	1.61
K_2O	4.21	5.76	5.78	4.92	6.06	5.35	0.77	2.5	3.97	3.29	5.22	1.75	4.37	2.16	3.85	3.39	1.19
TiO_2	0.49	0.38	0.41	0.07	0.38	0.35	0.16	0.07	0.05	0.05	0.04	0.08	0.06	0.05	0.06	0.06	0.01
P_2O_5	0.2	0.19	0.2	0.17	0.2	0.19	0.01	0.16	0.19	0.19	0.2	0.18	0.16	0.17	0.2	0.18	0.02
LOI	3.49	2.83	2.58	2.35	2.61	2.77	0.44	1.51	1.04	1	0.93	0.83	2.8	1.13	1.1	1.29	0.64
Total	100.43	100.31	100.00	99.89	99.98	100.12	0.23	100.28	100.14	99.7	100.18	100.85	98.97	100.26	99.9	100.04	0.54
Sc **ppm**	6	7	4	3	5	5	1.58	3	3	2	2	3	5	3	2	2.9	0.99
V	32	28	29	8	24	24.2	9.50	4	4	3	4	4	2	2	3	3.3	0.89
Cr	10	6	7	d.l.	8	7.75	1.71	0	0	0	0	0	1	0	0	0.1	0.35
Co	22	27	28	20	33	26	5.15	50	53	50	55	46	16	46	36	44.0	12.71
Ni	6	6	6	4	6	5.6	0.89	3	2	2	3	2	1	2	3	2.3	0.71
Cu	1	3	3	1	2	2	1.00	5	5	5	3	7	3	5	5	4.8	1.28
Zn	17	27	33	24	28	25.8	5.89	28	21	9	15	21	11	15	37	19.6	9.30
Ga	17.6	18	19	17	20	18.32	1.19	13	15	14.7	12	14.4	16	14	18	14.6	1.83
Rb	177	267	292	226	289	250.2	48.68	88	163	139	195	78	178	88	284	151.6	69.60
Sr	20	20	18	15	20	18.6	2.19	415	28	28	38	47	9	35	54	81.8	135.33
Y	16	20	21	5	20	16.4	6.66	25	6	8	6	6	8	8	6	9.1	6.49
Zr	165	139	159	23	142	125.6	58.40	23	17	17	14	25	23	21	31	21.4	5.40
Nb	15	14	15	5	14	12.6	4.28	7	8	11	6	9	8	6	21	9.5	4.93
Ba	128	285	223	193	270	219.8	63.10	116	25	14	31	162	107	48	35	67.3	53.82
Pb	4.6	5.6	5.3	3.8	6.5	5.16	1.02	246.6	34	43.2	68.4	16.5	4.2	32.6	26.9	59.1	78.10
Th	14.8	12.1	12.7	0.9	13.2	10.74	5.59	1.3	0	0	0	0.6	0	0.3	0.9	0.4	0.50
U	1.3	2.1	2.9	0.1	3.4	1.96	1.31	2.9	1.5	3.3	1.9	3.5	0	2.3	9.5	3.1	2.81
La	3	26	22	4	24	15.8	11.32	8	1	0	0	3	0	2	2	2.0	2.67
Ce	0	49	49	0	46	28.8	26.32	11	0	0	0	0	0	0	0	1.4	3.89
Pr	1	4	6	1	5	3.4	2.30	0	1	0	0	1	0	0	1	0.4	0.52
Nd	4	24	26	0	25	15.8	12.70	5	1	1	0	2	0	0	2	1.4	1.69
Sm	4	6	7	3	4	4.8	1.64	0	5	3	5	1	2	1	2	2.4	1.85

* Total Fe shown as Fe_2O_3; Fe^{2+}/Fe^{3+} not determined.

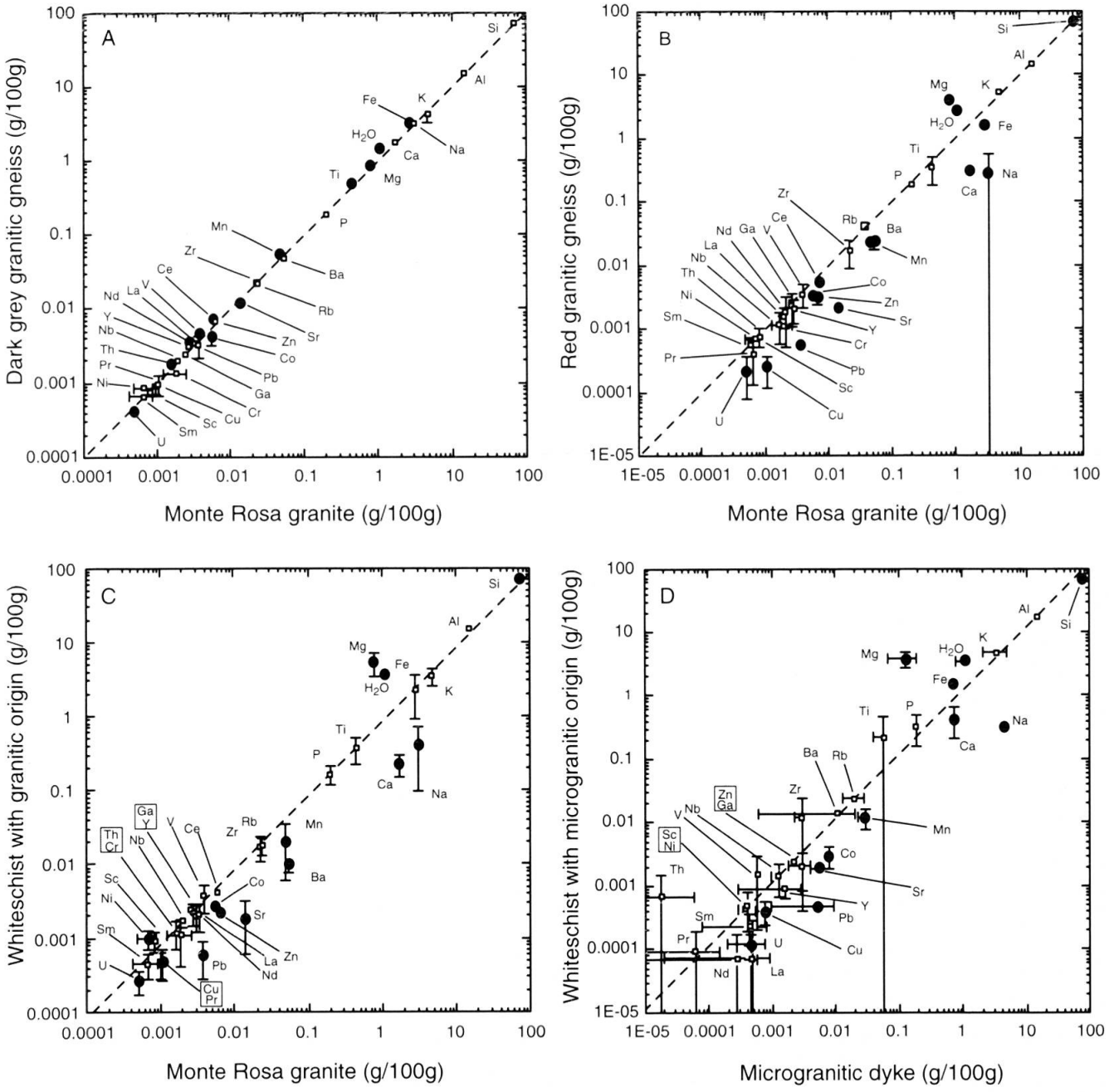

Fig. 5 Isocon diagrams displaying results of mass balance calculations: (A) alteration of the granite to dark variety of the granitic gneiss; (B) alteration to red variety of granitic gneiss; (C) alteration of granite to whiteschist with granitic origin; (D) alteration of micrograniticdyke to whiteschist with micrograniticorigin. Dashed line in each diagram is best fit ISOCON. Whole rock chemical data are given in table 1. Mobile elements in each diagram are indicated by filled circles; immobile elements are shown as open squares. Error bars were calculated from multiple samples, and indicate rock population variability.

ized by a gain in Mg and H_2O, as well as a decrease in concentration of Na, Ca, Sr, Ba, Mn, Fe, and several other trace elements including U, Pb and Ce. The eighteen elements compatible with the ISOCON for the alteration from the Monte Rosa granite to the red granitic gneiss are given in table 2. The overall mass gain of 2% is within the uncertainty of the mass ratio b = 0.98 ± 0.03.

Results of the mass balance calculation of the whiteschists with a granitic protolith are given in figure 5c, with 21 elements being compatible with the ISOCON (Tab. 2). Enrichment in Mg and H_2O and depletion in e.g. Na, Ca, Sr and Ba are indicated. An estimated overall mass gain of 17 ± 6 percent is shown graphically by the displacement of the ISOCON along the x-axis. Our analy-

Tab. 2 Combinations of immobile elements (x) compatible with the ISOCON. Mass balance calculations were done using the "ISOCON" software package (BAUMGARTNER and OLSEN, 1995). For each calculation, the ISOCON was chosen to have a maximum number of elements with generally assumed low-solubility (Al, Ti, P, Sc, Y, Zr, Nb, Th). Order of elements is similar to that in table 1. Note that the mobile elements are outlined.

Element	Monte Rosa granite to Dark granitic gneiss	Monte Rosa granite to Red granitic gneiss	Monte Rosa granite to Whiteschist	Microgranitic dyke to Whiteschist
Si	x			
Al	x	x	x	x
Fe			x	
Mn				
Mg				
Ca	x			
Na	x			
K	x	x	x	x
Ti		x	x	x
P	x	x	x	x
H_2O				
Sc	x	x	x	x
V		x	x	x
Cr	x	x	x	
Co				
Ni	x	x		x
Cu	x			
Zn	x			x
Ga	x	x	x	x
Rb	x	x	x	x
Sr				
Y	x	x	x	x
Zr	x	x	x	x
Nb	x	x	x	x
Ba	x			x
Th		x	x	x
Pb	x			
U				
La	x	x	x	x
Ce			x	
Pr	x	x		x
Nd		x	x	x
Sm	x	x	x	x

sis shows that 12 elements are mobile, whereby Mg, Na and Ca changed the most during the formation of the whiteschist.

Mass balance calculation of the alteration from the weakly deformed microgranitic dykes to the whiteschists with presumed microgranitic origin is shown in figure 5d, together with the ISOCON. The compatible elements are given in table 2. Again, a similar alteration pattern can be observed, with an enrichment in Mg, Fe and H_2O, whereas Na and Ca as well as Sr, Mn and Pb are strongly depleted (Fig. 5d). In contrast to the previous example, the displacement of the ISOCON in y-direction corresponds to a mass loss of 15 ± 9 percent during the alteration process, mainly due to the large silica loss.

Stable isotope geochemistry

The stable isotope compositions of carbon and oxygen of calcite from the carbonate zone located in the center of the shear zone were determined in order to constrain the possible origin of the fluids responsible for the hydrothermal alteration of the Monte Rosa granite. Three small samples (3 mm in diameter and 4 mm in depth) of the carbonate were drilled from sample 99SL124. They gave $\delta^{13}C_{PDB}$ values of –9.60 to –9.87‰ and $\delta^{18}O_{VSMOW}$ values of +9.48 to +10.14‰. Furthermore, two small samples (3 mm in diameter and 3 mm in depth) were drilled from the carbonate of sample 99SL144, which gave $\delta^{13}C_{PDB}$ values of –9.70 to –9.81‰ and $\delta^{18}O_{VSMOW}$ values of +9.61 to +9.82‰. In a diagram $\delta^{18}O_{VSMOW}$ versus $\delta^{13}C_{PDB}$, the values

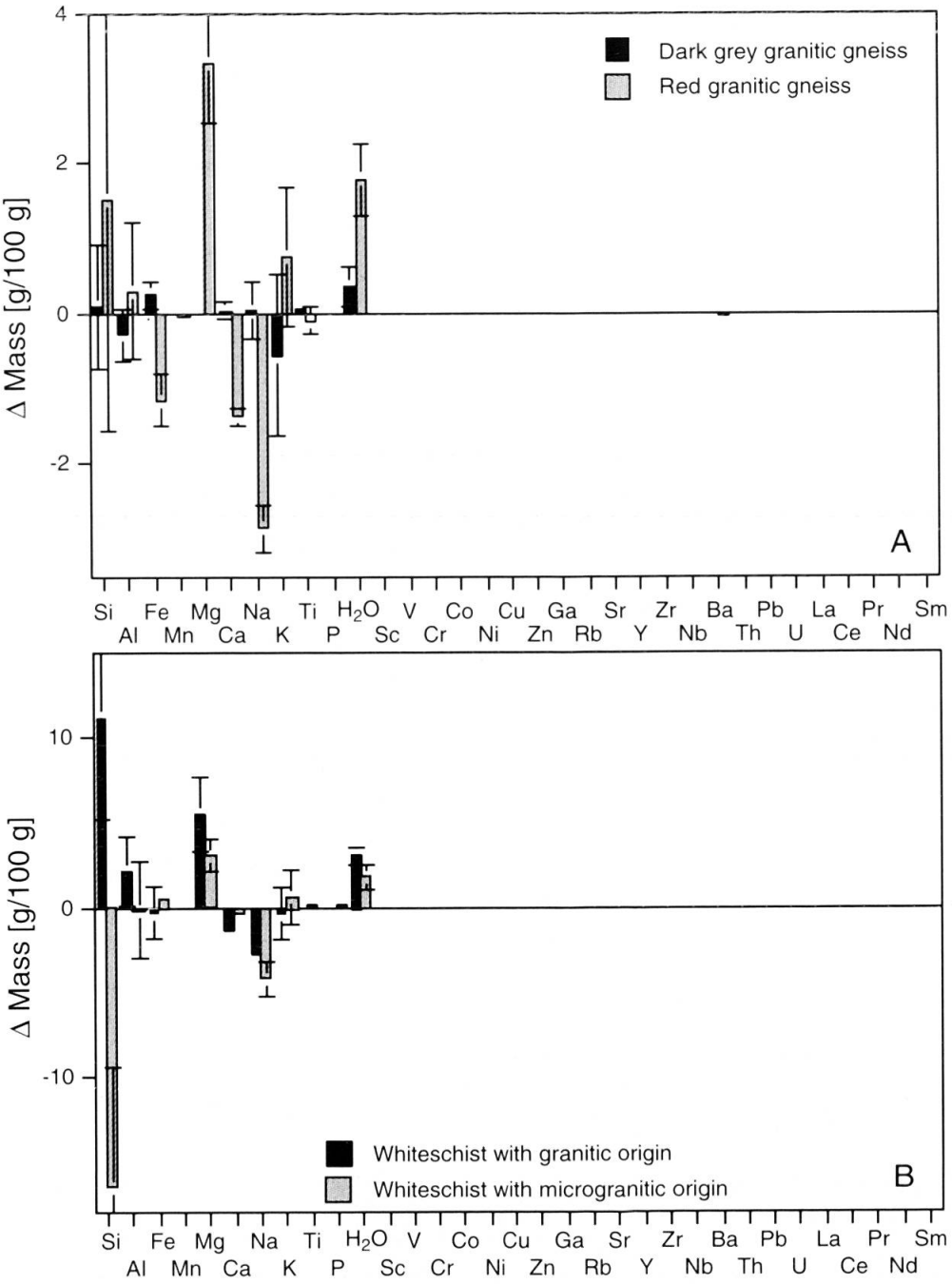

Fig. 6 Calculated mass changes in % for (A) mass gains and losses of elements for both varieties of the granitic gneiss formed from the granite and (B) mass changes for both whiteschist-types formed from the granite and the microgranitic dyke, respectively. The difference between the two alterations is restricted mainly to the silica leaching.

of the two analyzed samples fall into the field typical of magmatic fluids (Fig. 7; OHMOTO, 1986; SHEPPARD, 1986).

Discussion

From field evidence of the shear zone in the upper Val d'Ayas it is obvious that the protoliths for the whiteschists are the Monte Rosa granite and its microgranitic dykes. General geochemical characteristics of the alteration process from the Monte Rosa granite to the whiteschist are summarized in figure 6. The alteration increases towards the center of the shear zone. Mainly Mg, H_2O and to a lesser degree K, Si and Fe are enriched, while Ca, Na, Ba, Sr, Pb were leached from the Monte Rosa granite to form whiteschists. Hence, the fluid was characterized by a high activity of Mg, K and Si, but a low activity of Ca and Na. Initial chemical differences especially in the Si-content between the granitic and microgranitic protolith produce

Tab. 3 Stable isotope composition of carbon and oxygen of calcite from two samples of the carbonate boudin from the center of the shear zone.

Sample #	$\delta^{13}C_{PDB}$ ‰	$\delta^{18}O_{VSMOW}$ ‰
99SL124-1	–9.60	10.14
99SL124-2	–9.68	9.48
99SL124-3	–9.68	9.63
99SL144-1	–9.70	9.82
99SL144-2	–9.81	9.61

the apparent differences in the alteration process. Therefore, the difference between the two alterations is restricted mainly to the silica leaching for the production of whiteschists from their microgranitic dyke protoliths resulting from their initially present bulk chemical differences (Fig. 6b).

The composition of the Monte Rosa granite and its dykes is fairly homogeneous (Tab. 1; Fig. 5). Similarly, the compositions of the gneisses are still very homogeneous and only slightly altered, while the composition of the whiteschists varies widely. Hence, the compositional heterogeneity of the whiteschists is due to the alteration process, and alteration was heterogeneous. Thus uncorrelated statistics, as assumed by the calculations, is adequate to compare the granite compositions with those of whiteschists. In contrast, the homogeneity in the composition of the granitic gneiss is probably correlated to that of the unaltered, fairly homogenous granite population. The possible correlation of uncertainties of the gneiss population mainly influences the uncertainty estimate of the fit, not so much the location of the ISOCON. Nevertheless, the calculations show that mass transport is definitely small for the change from granite to granitic gneiss.

Metasomatic alteration leading to the shear zone rocks took place either prior to or during high-pressure metamorphism, since the high-pressure assemblages are restricted to the altered rocks. CHOPIN et al. (1991) and SHARP et al. (1993) argued for syn-high-pressure metasomatism in the Dora Maira massif. They call on metamorphic fluids escaping from the downgoing slab during metamorphism to produce similar whiteschist. Nevertheless, field and structural evidence for a pre-Alpine metasomatic alteration of the granite chemistry is given from occurrences of undeformed to slightly deformed whiteschists within the Monte Rosa granite near the Mezzalama refuge in the upper Val d'Ayas. In this area, the chloritoid-talc-bearing rocks with minor kyanite occur as patches, irregular zones, and vein like structures within the Monte Rosa granite. Microgranitic dykes can locally be traced into the whiteschists as ghost structures while others are totally obliterated by the whiteschists. All foliation discordantly cuts the contact between the Monte Rosa granite and the whiteschists. Thus, clear evidence is given that the metasomatic alteration took place prior to the Alpine metamorphism and deformation.

Magnesium-rich fluids can easily be produced by metamorphism of ultramafic and mafic rocks of the downgoing slab. These fluids might be potassium-rich, because some of the source rocks contain biotite and phengite. A decrease in temperature will eventually lead to silica saturation (EUGSTER and BAUMGARTNER, 1987) and silica precipitation. Such fluids will most likely have a light oxygen isotopic signature, in agreement with those measured also for the Monte Rosa shear zone. From a structural point of view, KELLER and SCHMID (2001) argue for a development of shear zones within the Monte Rosa nappe during Alpine eclogite-facies metamorphism. However, we prefer a pre-high-pressure metamorphic origin of the whiteschist chemistry, because of the light carbon isotopic values ($\delta^{13}C$ from –9.60 to –9.87‰) measured in calcite from the carbonate zone in the center of the shear zone. Those light isotopic values for carbon are difficult to explain

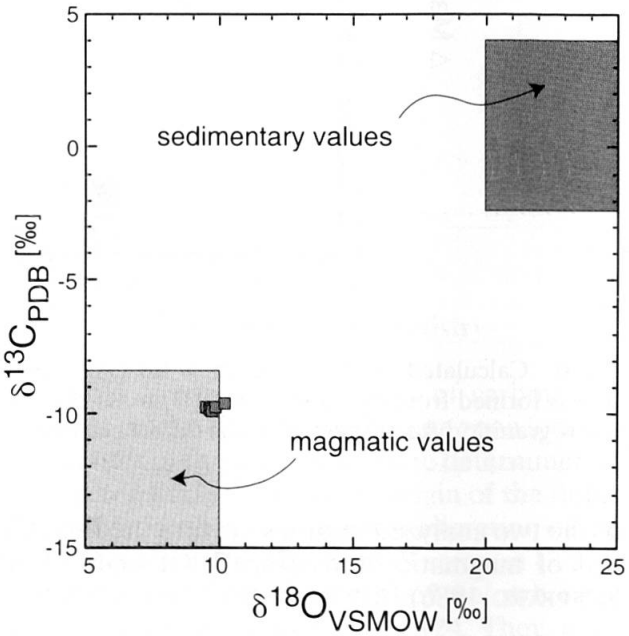

Fig. 7 The $\delta^{18}O_{VSMOW}$ and $\delta^{13}C_{PDB}$ values of calcite bearing samples from the carbonate boudin located within the center of the shear zone. Unusual, light oxygen and carbon values are most similar to igneous compositions. Values for reference fields of magmatic and sedimentary stable isotope signatures from VALLEY et al. (1986) and HOEFS (1987).

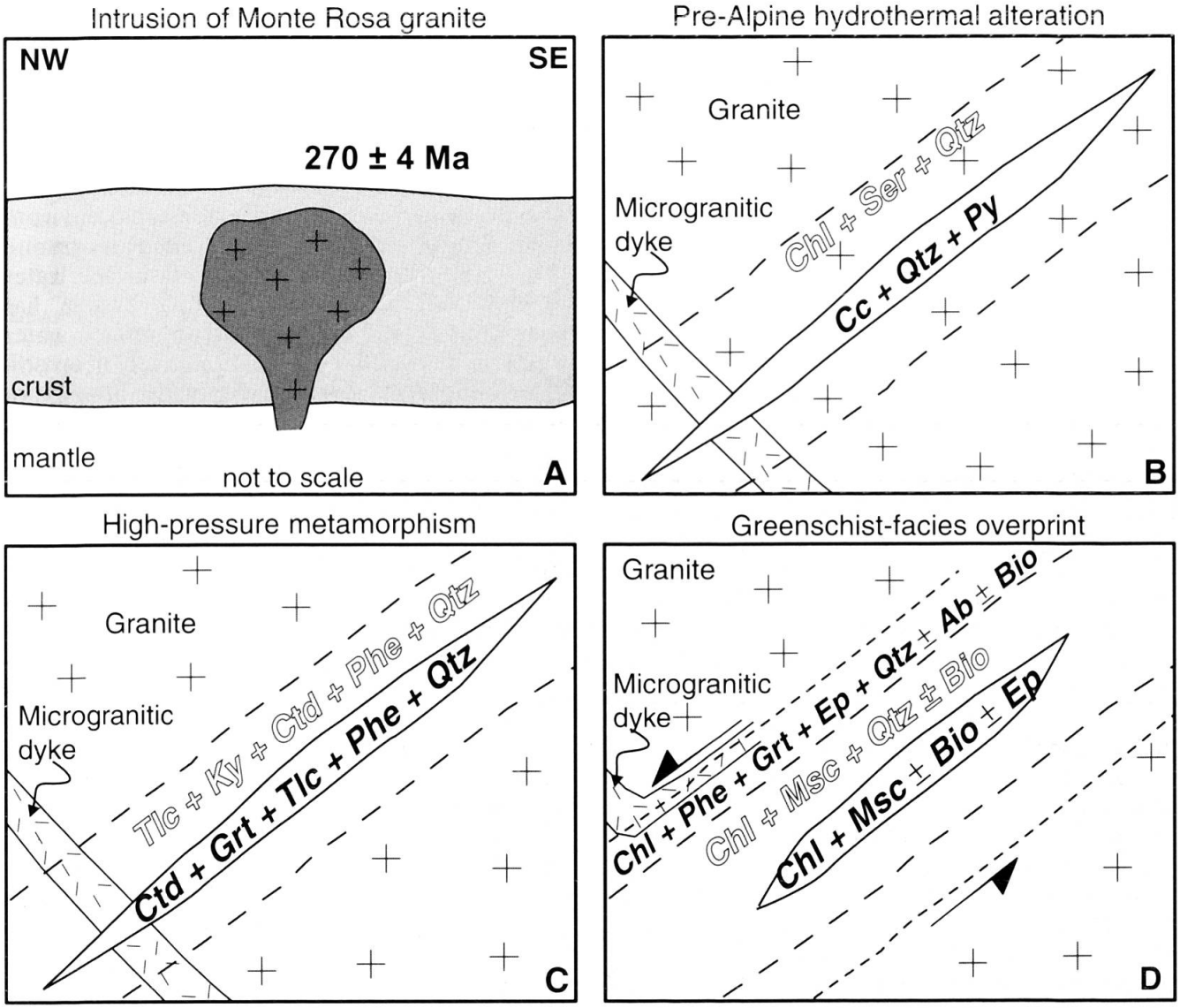

Fig. 8 Schematic model (not to scale) of geochemical and structural evolution of the shear zone in the upper Val d'Ayas, Italy. (A) Permian intrusion of the Monte Rosa granite (PAWLIG et al., submitted; ENGI et al., 2001). (B) Formation of Mg-rich bulk composition within the Monte Rosa granite occurred during late-stage, hydrothermal fluid activity along veins. These were filled with gangue assemblage calcite-quartz-pyrite-chalcopyrite. (C) Alpine high-pressure metamorphism causes formation of whiteschists with assemblage talc-kyanite-chloritoid-phengite-quartz from the chlorite-rich, altered granitic protolith. The assemblage chloritoid-garnet-talc-phengite-quartz develops in the vein filling. (D) Strain localization during subsequent exhumation continued well into the greenschist-facies overprint.

by metasomatic alteration due to metamorphic fluids, since possible source rocks for the carbon are sedimentary rocks, either of the Monte Rosa cover sequence or the Zermatt-Saas Zone, and those low $\delta^{13}C$ values would require organic carbon-rich pelites. No graphite-bearing rocks as potential carbon-source have been reported from the Monte Rosa cover sequence (DAL PIAZ, pers. comm.). Parts of the Zermatt-Saas Zone were subducted to greater pressures than the Monte Rosa nappe (REINECKE, 1998; AMATO et al., 1999) and are thus potential source rocks for fluids, but oceanic sediments produce much heavier carbon isotope compositions than observed here (OHMOTO, 1986; SHEPPARD, 1986; VALLEY, 1986; HOEFS, 1987). Another potential fluid sources are ophicarbonates from the overlying Zermatt-Saas Zone. Studies on ophicarbonates from different units in the Penninic realm, on the high-pressure/low-temperature ophiolite of Corsica (France) and of high-pressure metamorphic marbles from Tinos (Cyclades, Greece) show heavy values for the $\delta^{13}C$ (–6.3 to +3‰). This reflects the marine origin of the carbonate (WEISSERT and BERNOULLI, 1984; BURKHARD and O'NEIL, 1988; FRÜH-GREEN et al., 1990; DRIESNER, 1993; GANOR et al.,

1994; POZZORINI and FRÜH-GREEN, 1996; MATTHEWS et al., 1999; CARTWRIGHT and BUICK, 2000; MILLER et al., 2001). The $\delta^{18}O$ of calcite from the Corsican ophiolite sequence varies between +11.1 and +22.9‰ (Miller et al., 2001). They are similar to $\delta^{18}O$ values of Corsican schistes lustrés (CARTWRIGHT and BUICK, 2000), and imply the derivation of the calcite from sedimentary derived fluids (MILLER et al., 2001). In fact, if the carbon of the Monte Rosa shear zone precipitated due to infiltration of a fluid derived from calcareous metasediments (i.e. schistes lustrés) during high-pressure metamorphism, the expected $\delta^{13}C$ values of carbonate should be around 0‰, or even a mixture between magmatic and sedimentary $\delta^{13}C$. It is thus very difficult to produce the observed carbon isotope signature in the carbonate zone from fluids evolving from a subducted oceanic slab with accompanied oceanic sediments. Another interesting aspect of the ophiolitic high-pressure rocks of the Zermatt-Saas unit is, that many of the eclogites and blueschists are extremely sodium-rich (GANGUIN, 1988) due to fluid interaction during ocean-floor metamorphism. Fluids evolving from these eclogites and blueschists would most likely be quite sodium-rich, which could lead to sodium enrichment, rather than the observed depletion.

Therefore, the most likely cause of metasomatism leading to the precursors of the whiteschists is that of a late magmatic, hydrothermal alteration, which took place prior to Alpine metamorphism. $\delta^{13}C$ values for hydrothermal gangue carbonate in ore deposits ranging from –6 to –9‰ are quite common (OHMOTO and RYE, 1979; OHMOTO, 1986). The observed assemblage carbonate-quartz-sulfide (pyrite/chalco-pyrite) of the Monte Rosa shear zone is common in such rocks. Hence, the carbonate zone represents a late magmatic vein mineralization within the Monte Rosa granite (Figs 7 and 4b). In particular, argillitic and potassic alteration (e.g. MEYER and HEMLEY, 1967) in a magmatic environment leads to the formation of chlorite-rich, potassium-rich rocks, which chemically are similar to the precursor for the whiteschists. No alteration of the magmatic stable isotopic signature of carbon and oxygen during Alpine metamorphic evolution has taken place. Thus, it is suggested that the shear zone has not been infiltrated by significant amounts of fluids during its Alpine metamorphic history.

Based on the above discussion, we suggest the following model for the formation of the Monte Rosa whiteschists (Fig. 8). The Monte Rosa granite intruded the high-grade metapelitic basement during Permian times (270 ± 4 Ma, PAWLIG et al., subm.; ENGI et al., 2001; Fig. 8a). The assemblage calcite-quartz-sulfide developed as a vein mineralization during late magmatic hydrothermal fluid activity of the Permian Monte Rosa granite. The hydrothermal fluid activity was probably related to post-Variscan processes as a consequence of post-orogenic uplift and extension (FINGER et al., 1997; PAWLIG et al., subm.). Juvenile fluids escaping in this extensional environment altered the surrounding Monte Rosa granite (Fig. 8b). So far, no indication of surface water precipitation in the hydrothermal system has been found. This implies that no surface water was available, either due to a relatively deep emplacement level of the pluton or the absence of significant surface waters. Those fluids caused the formation of chlorite- and sericite-rich assemblages from the granitic protolith, whereas calcium and sodium were leached. The presence of pre-existing hydrous minerals in the metasomatized zone and the mineral chemistry promoted the formation of the assemblage kyanite-talc-Mg-chloritoid within this zone during the Alpine high-pressure metamorphic overprint. The surrounding granite maintained its mostly igneous mineralogy due to dry conditions (Fig. 8c). The whiteschists might have helped to localize the shear zone. Protracted deformation during exhumation resulted in a partial greenschist-facies overprint of the whiteschists. The shear zone probably remained active or was reactivated during the subsequent greenschist-facies Alpine metamorphism (Fig. 8d).

Acknowledgements

This research was supported by the German Science Foundation (Graduiertenkolleg GK392/1). S.P. would like to thank N. Groschopf for performing the XRF analyses. W. Lackmann kindly helped with the stable isotope measurements. This paper has benefitted from discussions and useful comments on earlier drafts by S. Piazolo and A. Möller. The constructive discussions during the Monte Rosa field trip of the Swiss Mineralogical Society as well as the thoughtful reviews by A. Matthews and M. Engi are greatfully acknowlegded and helped to significantly improve the manuscript.

References

ABRAHAM, K., HÖRMANN, P. and RAITH, M. (1974): Progressive metamorphism of basic rocks from the southern Hohe Tauern area, Tyrol (Austria). N. Jb. Mineral. Abh. 122, 1–35.

AGUE, J.J. (1994): Mass transfer during Barrovian metamorphism of pelites, south-central Conneticut; I, Evidence for changes in composition and volume. Am. J. Sci. 294, 989–1057.

AGUE, J.J. (1997): Compositional variations in metamorphosed sediments of the Littleton Formation, New Hampshire; discussion. Am. J. Sci. 297, 440–449.

AMATO, J.M., JOHNSON, C.M., BAUMGARTNER, L.P. and BEARD, B.L. (1999): Rapid exhumation of the Zermatt-Saas ophiolite deduced from high precision Sm–Nd and Rb–Sr geochronology. Earth Planet. Sci. Lett. 171, 425–438.

BARNICOAT, A. and CARTWRIGHT, I. (1995): Focused fluid flow during subduction: Oxygen isotope data from high-pressure ophiolites of the western Alps. Earth Planet. Sci. Lett. 132, 53–61.

BAUMGARTNER, L.P. and OLSEN, S.N. (1995): A least-squares approach to mass transport calculations using the ISOCON method. Econ. Geol. 90, 1261–1270.

BEARTH, P. (1952): Geologie und Petrographie des Monte Rosa. Beitr. Geol. Karte Schweiz NF 96, 94 pp.

BURKHARD, D. and O'NEIL, J. (1988): Contrasting serpentinization process in the eastern Central Alps. Contrib. Mineral. Petrol. 99, 498–506.

CARTWRIGHT, I. and BUICK, I.S. (2000): Fluid generation, vein formation and the degree of fluid-rock interaction during decompression of high-pressure terranes: the Schistes Lustrés, Alpine Corsica, France. J. Metamorphic Geol. 18, 607–624.

CHOPIN, C. and MONIÉ, P. (1984): A unique magnesiochloritoid-bearing, high-pressure assemblage from the Monte Rosa, Western Alps; petrologic and ^{40}Ar–^{39}Ar radiometric study. Contrib. Mineral. Petrol. 87, 388–398.

CHOPIN, C., HENRY, C. and MICHARD, A. (1991): Geology and petrology of the coesite-bearing terrain, Dora Maira massif, Western Alps. Eur. J. Mineral. 3, 263–291.

DAL PIAZ, G.V. (1971): Nuovi ritrovamenti di cianite alpina nel cristallino antico del Monte Rosa. Rend. Soc. Ital. Mineral. Petrol. 27, 437–477.

DAL PIAZ, G.V. and LOMBARDO, B. (1986): Early Alpine eclogite metamorphism in the Penninic Monte Rosa-Gran Paradiso basement nappes of the northwestern Alps. Geol. Soc. Am. Mem. 164, 249–265.

DEMÈNY, A., SHARP, Z. and PFEIFER, H.R. (1997): Mg-metasomatism and formation conditions of Mg-chlorite-muscovite-quartzphyllites (leucophyllites) of the Eastern Alps (W. Hungary) and their relations to Alpine whiteschists. Contrib. Mineral. Petrol. 128, 247–260.

DRIESNER, T. (1993): Aspects of petrographical, structural and stable isotope geochemical evolution of ophicarbonate breccias from ocean floor to subduction and uplift: an example from Chatillon, Middle Aosta Valley, Italian Alps. Schweiz. Mineral. Petrogr. Mitt. 73, 69–84.

ENGI, M., SCHERRER, N.C. and BURRI, T. (2001): Metamorphic evolution of pelitic rocks of the Monte Rosa nappe: Constraints from petrology and single grain monazite age data. Schweiz. Mineral. Petrogr. Mitt. 81, 305–328.

EUGSTER, H.P. and BAUMGARTNER, L.P. (1987): Mineral solubilities and speciation in supercritical metamorphic fluids. In: CARMICHAEL, I.S.E. and EUGSTER, H.P. (eds): Thermodynamic modeling of geological materials: Minerals, fluids and melts. Reviews in Mineralogy 17, 367–403

FAURE, G. (1986): Principles of isotope geology. 2nd edition, John Wiley and Sons, New York, 589 pp.

FINGER, F., ROBERTS, M.P., HAUNSCHMID, B., SCHERMAIER, A. and STEYRER, H.P. (1997): Variscan granitoids of central Europe: their typology, potential sources and tectonothermal relations. Mineral. Petrol. 61, 67–96.

FREY, M., HUNZIKER, J.C., O'NEIL, J.R. and SCHWANDER, H.W. (1976): Equilibrium-Disequilibrium Relations in the Monte Rosa Granite, Western Alps: Petrological, Rb–Sr and Stable Isotope Data. Contrib. Mineral. Petrol. 55, 147–179.

FRÜH-GREEN, G., WEISSERT, H. and BERNOULLI, D. (1990): A multiple fluid history recorded in Alpine Ophiolites. J. Geol. Soc. London 147, 959–970.

GANOR, J., MATTHEWS, A. and SCHLIESTEDT, M. (1994): Post metamorphic low $\delta^{13}C$ calcite veins in the Cycladic complex (Greece) and their implications for modeling fluid infiltration processes using carbon isotope composition. Eur. J. Mineral. 6, 365–379.

GANGUIN, J. (1988): Contribution à la caractérisation du métamorphisme polyphase de la zone de Zermatt-Saas Fee (Alpes Valaisannes). Ph.D. thesis, ETH Zürich.

GRANT, J.A. (1986): The ISOCON diagram – A simple solution to Gresens' equation for metasomatic alteration. Econ. Geol. 81, 1976–1982.

GRESENS, R.L. (1967): Composition-volume relationships of metasomatism. Chem. Geol. 2, 47–65.

HOEFS, J. (1987): Stable isotope geochemistry. 2nd ed. Springer, Berlin, 241 pp.

KELLER, L.M. and SCHMID, S.M. (2001): On the kinematics of shearing near the top of the Monte Rosa nappe and the nature of the Furgg zone in Val Loranco (Antrona valley, N. Italy): tectonometamorphic and paleogeographic consequences. Schweiz. Mineral. Petrogr. Mitt. 81, 347–367.

LE BAYON, R., DE CAPITANI, C., CHOPIN, C. and FREY, M. (2000): Modelling of the sequentional evolution of whiteschist assemblages: HP in the Monte Rosa (Western Alps). Beih. Eur. J. Mineral. 12, 111.

MATTHEWS, A., LIEBERMAN, J., AVIGAD, D. and GARFUNKEL, Z. (1999): Fluid-rock interaction and thermal evolution during thrusting of an Alpine metamorphic complex (Tinos Island, Greece). Contrib. Mineral. Petrol. 135, 212–224.

MEYER, C. and HEMLEY, J.J. (1967): Wall rock alteration. In: BARNES, H.L. (ed.): Geochemistry of hydrothermal ore deposits. Holt, Rinehart and Winston, New York, 166–235.

MILLER, J.A., CARTWRIGHT, I., BUICK, I.S. and BARNICOAT, A.C. (2001): An O-isotope profile through the HP-LT Corsican ophiolite, France and its implications for fluid flow during subduction. Chem. Geol. 178, 43–69.

OHMOTO, H. (1986): Stable isotope geochemistry of ore deposits. In: VALLEY, J.W., TAYLOR, H.P. JR. and O'NEIL, J.R. (eds): Stable isotopes in high temperature geological processes. Reviews in Mineralogy 16, 491–559.

OHMOTO, H. and RYE, R.O. (1979): Isotopes of sulfur and carbon. In: BARNES, H.L. (ed.): Geochemistry of hydrothermal ore deposits. 2nd ed., John Wiley and Sons, New York, 509–567.

OLSEN, S.N. and GRANT, J.A. (1991): ISOCON analysis of migmatization in the Front Range, Colorado, USA. J. Metamorphic Geol. 9, 151–164.

PAWLIG, S., POLLER, U., BAUMGARTNER, L.P. and TODT, W.: New U–Pb data on the crystallization age of the Monte Rosa granite, Western Alps – a combined SHRIMP, TIMS and cathodoluminescence study. Submitted to Eur. J. Mineral.

POZZORINI, D. and FRÜH-GREEN, G.L. (1996): Stable isotope systematics of the Ventina Ophicarbonate Zone, Bergell contact aureole. Schweiz. Mineral. Petrogr. Mitt. 76, 549–564.

REINECKE, T. (1998): Prograde high- to ultrahigh-pressure metamorphism and exhumation of oceanic sediments at Lago di Cignana, Zermatt-Saas Zone, western Alps. Lithos 42, 147–189.

SCHREYER, W. (1974): Whiteschist, a new type of metamorphic rock formed at high pressures. Geol. Rdschau. 63, 597–609.

SHARP, Z., ESSENE, E. and HUNZIKER, J. (1993): Stable isotope geochemistry and phase equilibria of coesite-bearing whiteschist, Dora Maira Massif, western Alps. Contrib. Mineral. Petrol. 114, 1–12.

SHEPPARD, S.M.F. (1986): Characterization and isotopic variations in natural waters. In: VALLEY, J.W., TAYLOR, H.P. JR. and O'NEIL, J.R. (eds): Stable isotopes in high temperature geological processes. Reviews in Mineralogy 16, 165–183.

SCHERRER, N.C. (2001): Behaviour of monazite and evolution of polymetamorphic pelites from the Monte Rosa Nappe, Western Central Alps, Italy. PhD thesis, Bern, 66 pp.

VALLEY, J.W. (1986): Stable isotope geochemistry of metamorphic rocks. In: VALLEY, J.W., TAYLOR, H.P. JR. and O'NEIL, J.R. (eds): Stable isotopes in high temperature geological processes. Reviews in Mineralogy 16, 445–489.

WEISSERT, H. and BERNOULLI, D. (1984): Oxygen isotope composition of calcite in ophicarbonates, a hydrothermal or Alpine metamorphic signal? Eclogae geol. Helv. 77, 29–43.

Manuscript received March 12, 2001; revision accepted September 30, 2001.